Akt3 kinase suppresses pinocytosis of low-density lipoprotein by macrophages via a novel WNK/SGK1/Cdc42 protein pathway

Liang Ding[‡], **Lifang Zhang**[‡], **Michael Kim**[§], **Tatiana Byzova**[‡], and **Eugene Podrez**[‡1]

From the ‡Department of Molecular Cardiology, Cleveland Clinic, Cleveland, Ohio 44195 and the §Department of Biochemistry, Case Western Reserve University, Cleveland, Ohio 44106

Edited by Thomas Söllner

Fluid-phase pinocytosis of LDL by macrophages is regarded as a novel promising target to reduce macrophage cholesterol accumulation in atherosclerotic lesions. The mechanisms of regulation of fluid-phase pinocytosis in macrophages and, specifically, the role of Akt kinases are poorly understood. We have found previously that increased lipoprotein uptake via the receptor-independent process in Akt3 kinase-deficient macrophages contributes to increased atherosclerosis in $Akt3^{-/-}$ mice. The mechanism by which Akt3 deficiency promotes lipoprotein uptake in macrophages is unknown. We now report that Akt3 constitutively suppresses macropinocytosis in macrophages through a novel WNK1/SGK1/Cdc42 pathway. Mechanistic studies have demonstrated that the lack of Akt3 expression in murine and human macrophages results in increased expression of with-no-lysine kinase 1 (WNK1), which, in turn, leads to increased activity of serum and glucocorticoid-inducible kinase 1 (SGK1). SGK1 promotes expression of the Rho family GTPase Cdc42, a positive regulator of actin assembly, cell polarization, and pinocytosis. Individual suppression of WNK1 expression, SGK1, or Cdc42 activity in Akt3-deficient macrophages rescued the phenotype. These results demonstrate that Akt3 is a specific negative regulator of macropinocytosis in macrophages.

Professional phagocytes such as macrophages constantly probe the extracellular milieu for foreign agents. Although larger particles are engulfed by phagocytosis, the soluble material and small particles are internalized by fluid-phase pinocytosis. Pinocytosis includes macropinocytosis, proceeding via membrane ruffling and formation of large vacuoles, and micropinocytosis, occurring via membrane invagination and subsequent pinching of small vesicles. Phagocytosis and macropinocytosis are driven by actin polymerization initiated by activation of the Rho-family GTPases (1). Micropinocytosis, on the other hand, may be actin-dependent or -independent (2, 3). The membrane ruffling that underlies macropinosome formation occurs continuously, in contrast to phagocytosis, which is believed to be a receptor-initiated process (4). Although phagocytosis and pinocytosis are part of the innate immune system, under conditions of hyperlipidemia, they can contribute to macrophage lipoprotein uptake and cholesterol accumulation, an early critical step in atherogenesis (5).

LDL is the major source of lipids for macrophage foam cell formation. Macrophage uptake of LDL occurs via scavenger receptor-mediated uptake of modified LDL and via receptor-independent processes (6, 7). Receptor-independent fluid-phase pinocytosis recently attracted significant attention because this process does not require LDL to be modified, but it can still lead to cholesterol accumulation to levels characteristic of foam cells in atherosclerotic plaques. More than 95% uptake of unmodified LDL by murine macrophages is accounted by macropinocytosis and micropinocytosis (8). Both types of pinocytosis substantially contribute to LDL uptake and cholesterol accumulation in human and murine macrophages (9). Almost all micropinocytotic uptake of LDL occurs in an actin-dependent manner (9), indicating that actin assembly plays a pivotal role in pinocytosis of LDL by macrophages. Importantly, it has been demonstrated that fluid-phase pinocytosis by macrophages occurs within mouse atherosclerotic plaques, indicating that this pathway contributes to macrophage cholesterol accumulation *in vivo* (10). Induction of constitutive pinocytosis because of activation of Rac1, Cdc42, and Rho has been shown to increase atherosclerosis in receptor-interacting protein 2 (Rip2)-deficient mice (11, 12). Consequently, fluid-phase pinocytosis of LDL by macrophages is regarded as a novel promising target to reduce macrophage cholesterol accumulation in atherosclerotic lesions (10, 13).

Mechanisms regulating pinocytosis in macrophages are complex and incompletely understood. Stimulation of pinocytosis requires activation of the PI3K/Akt pathway in some but not all cells (14, 15). PI3K/Akt positively regulates actin filament remodeling, a key element of pinocytosis (16, 17). Three Akt isoforms, encoded by three separate genes, are expressed in mammals. All three isoforms are expressed in macrophages; however, the role of individual forms of Akt in macrophage function is only starting to emerge (18, 19). Phenotypic analysis of the deletion of individual Akt isoforms and combined dele-

tions in the mouse suggests that isoforms may play compensatory as well as complementary roles (20). However, evidence accumulates that isoforms may have distinct functions, even at the cellular level (21).

Akt3 is reported to mainly participate in brain development, neurological function, and specific types of cancer (22). Our recent study demonstrated that the lack of Akt3 expression in macrophages promotes atherosclerosis via increased accumulation of cholesterol via enhanced receptor-independent uptake of LDL and increased expression of ACAT1 by these cells (21). In this study, we explored the mechanism of increased uptake of LDL in $Akt3^{-/-}$ macrophages. We found that Akt3 controls a novel pathway of actin-dependent macropinocytosis in macrophages by suppressing the expression of WNK[2] and activity of SGK1, two kinases that have not been implicated previously in pinocytosis. We further demonstrated that increased activity of SGK1 leads to activation of Cdc42-dependent actin assembly and promotes lipoprotein uptake via macropinocytosis.

Results

Akt3 deficiency leads to increased uptake of LDL via macropinocytosis in murine and in human macrophages

In agreement with our previous study (21), we observed increased uptake of Lucifer yellow dye by $Akt3^{-/-}$ macrophages, indicating increased fluid phase uptake (Fig. 1*A*). We hypothesized that Akt3 deficiency in macrophages will lead to increased uptake of LDL via the pinocytotic pathway. To test this hypothesis, we cultured murine peritoneal macrophages (MPMs) isolated from wild type and $Akt3^{-/-}$ mice with high concentrations of ^{125}I-LDL (100 μg/ml), which allowed us to detect uptake of LDL via nonspecific processes such as pinocytosis. We observed enhanced uptake of ^{125}I-LDL by $Akt3^{-/-}$ MPMs (Fig. 1*B*). To investigate whether loss of Akt3 directly contributes to the phenotype of $Akt3^{-/-}$ MPMs, we transfected $Akt3^{-/-}$ MPMs with Akt3 cDNA. Western blot analysis showed adequate expression of both the HA tag and Akt3 in $Akt3^{-/-}$ MPMs transfected with Akt3 cDNA (Fig. 1*C*). The transfection efficiency in these experiments assessed using antibody against HA reached 51.4% (Fig. 1*D*). The phenotype of $Akt3^{-/-}$ MPMs was partially rescued by overexpression of Akt3 in these cells (Fig. 1, *E* and *F*). To test whether downregulation of Akt3 expression would affect pinocytosis in human macrophages in a similar manner, we performed Akt3 knockdown in human monocyte-derived macrophages (MDMs) by siRNA approach. Western blot analysis confirmed significant inhibition of Akt3 expression by Akt3-specific siRNA (Fig. 1*G*). Akt3 suppression was associated withtk;1 enhanced cholesterol accumulation in human MDMs incubated with LDL, suggesting that enhanced pinocytosis may significantly contribute to foam cell formation (Fig. 1*H*). Taken together, these results demonstrate that a lack of Akt3

expression activates pinocytosis in murine and human macrophages.

Fluid-phase pinocytosis can occur by either micropinocytosis or macropinocytosis, and both processes may depend on actin polymerization (9). To test which process is activated in $Akt3^{-/-}$ macrophages and whether this process is actin-dependent, we performed a pinocytosis assay using WT and $Akt3^{-/-}$ MPMs in the presence of an Src family kinase inhibitor (SU6656), vacuolar H^+-ATPase inhibitor (bafilomycin A1), or an inhibitor of actin polymerization (cytochalasin D). It has been reported that SU6656 inhibits macrophage macropinocytosis, whereas bafilomycin A1 inhibits micropinocytosis but not macropinocytosis (9) (supplemental Fig. S1*C*). SU6656 and cytochalasin D abolished increased pinocytosis in $Akt3^{-/-}$ macrophages (Fig. 2*A*), suggesting that a loss of Akt3 in MPMs stimulates actin-dependent macropinocytosis but not micropinocytosis. Furthermore, cholesterol accumulation in human MDM with suppressed expression of Akt3 was inhibited by SU6656 and cytochalasin D (Fig. 2*B*).

Akt3$^{-/-}$ macrophages display no increase in expression or activity of Akt1/Akt2

Akt is a known regulator of actin-dependent macropinocytosis (23). Akt1 and Akt2 regulate actin filament formation by either inhibiting or promoting actin assembly and rearrangement (24). To test whether Akt1 and/or Akt2 are responsible for enhanced actin-dependent macropinocytosis in $Akt3^{-/-}$ MPMs, we assessed Akt expression and phosphorylation status in these cells. Phosphorylation of Akt in macrophages was induced by M-CSF, a cytokine that plays an essential role in monocyte-macrophage functions, including pinocytosis, cell migration, chemotaxis, and cytokine production. We observed slightly decreased phosphorylation of Akt (Ser-473/Thr-308) as well as mildly reduced total Akt expression in $Akt3^{-/-}$ MPMs, which likely reflects a loss of Akt3 expression (Fig. 3*A*). No change in Akt1 and Akt2 expression was found in $Akt3^{-/-}$ MPMs (Fig. 3*A*), ruling out increased expression or activation of Akt1/Akt2 as a mechanism for increased pinocytosis and actin assembly. We also tested whether increased pinocytosis in $Akt3^{-/-}$ MPMs depends on major downstream molecules of the Akt signaling pathway, such as mechanistic target of rapamycin (mTOR), glycogen synthase kinase 3, and NFκB. We observed a significant change in pinocytosis of $Akt3^{-/-}$ MPMs after treatment with the inhibitors of the abovementioned pathways (Fig. 3*B*), again indicating that Akt1/2 expression activity is not responsible for enhanced pinocytosis in $Akt3^{-/-}$ macrophages.

Enhanced activity of SGK1 promotes pinocytosis in Akt3$^{-/-}$ murine peritoneal macrophages

SGK1 kinase belongs to the AGC (protein kinase A, G, and C) family of kinases and shares the upstream activation pathways and consensus phosphorylation motif with Akt (25–27). A lack of Akt can be compensated in some cells by elevated SGK1 (28). We hypothesized that SGK1 may have a role in increased pinocytosis in $Akt3^{-/-}$ macrophages. The SGK1 protein level was not significantly changed in $Akt3^{-/-}$ MPMs (Fig. 3*C*, *top panels*). However, phosphorylation of NDRG1, an SGK1-spe-

---

[2] The abbreviations used are: WNK, with-no-lysine kinase; MPM, murine peritoneal macrophage; MDM, monocyte-derived macrophage; mTOR, mechanistic target of rapamycin; TRITC, tetramethylrhodamine isothiocyanate; SGK, serum- and glucocorticoid-inducible kinase; SGK1i, SGK1 inhibitor.
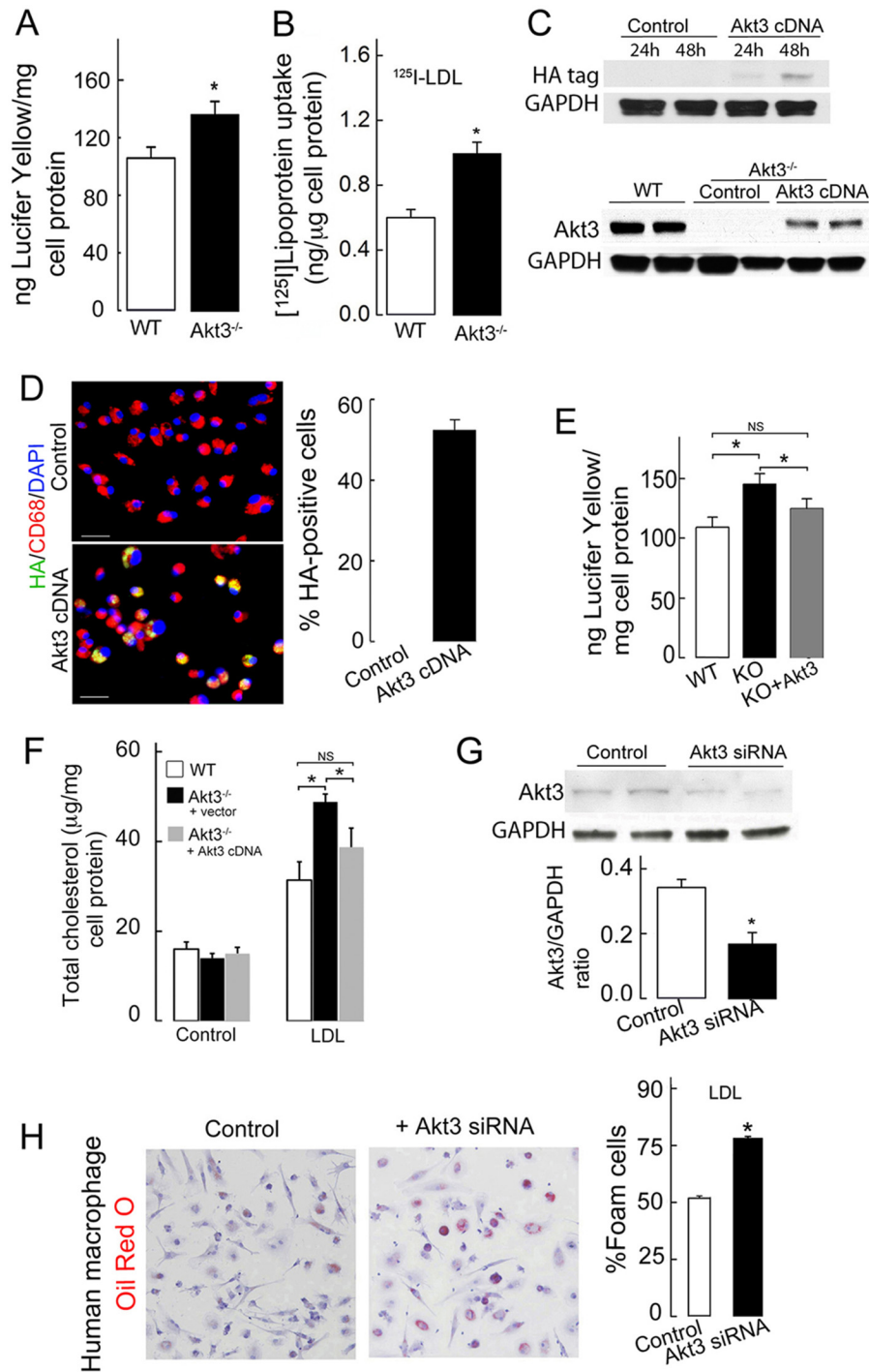
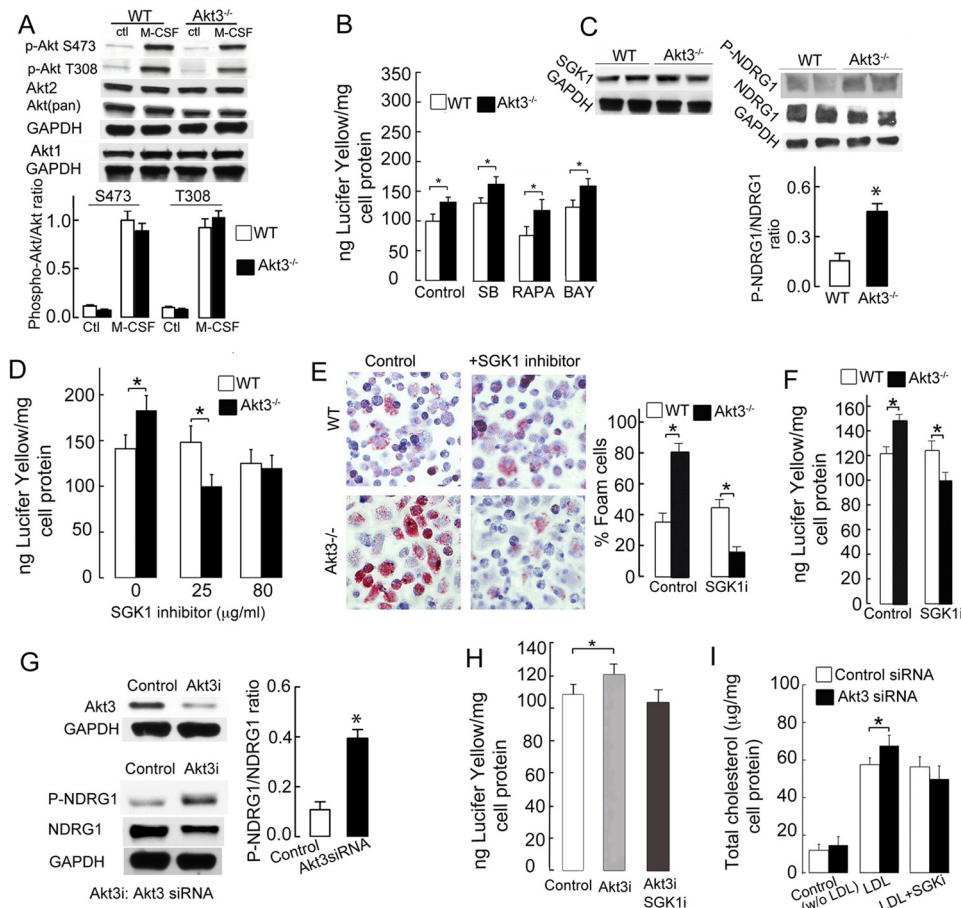**Figure 1. Suppression of Akt3 expression in murine and human macrophages promotes pinocytosis.** *A*, uptake of Lucifer yellow dye by WT and *Akt3*$^{-/-}$ MPMs. Wild-type or *Akt3*$^{-/-}$ MPMs were cultured in RPMI 1640/10% FBS medium containing 0.5 mg/ml Lucifer yellow dye at 4 °C or at 37 °C for 2 h. Cells were washed, lysed by Triton X-100, and Lucifer yellow was quantified by spectrofluorometry (*n* = 6). *B*, uptake of ^{125}I-LDL by WT and *Akt3*$^{-/-}$ MPMs. MPMs from WT and *Akt3*$^{-/-}$ mice were incubated for 8 at 37 °C with 100 μg/ml of ^{125}I-labeled native LDL, and uptake of ^{125}I-lipoprotein was quantified (*n* = 5). *C*, expression of the HA tag (*top panel*) or Akt3 (*bottom panel*) in WT or *Akt3*$^{-/-}$ MPMs transfected with a control plasmid or a plasmid containing Akt3 cDNA (*top panel*) (*n* = 3). *D*, *Akt3*$^{-/-}$ MPMs were stained with antibodies against the HA tag (*green*), the macrophage marker CD68 (*red*), and with DAPI (*blue*) after transfection with control vector or plasmid containing Akt3 cDNA for 48 h (*n* = 8). *Scale bars* = 25 μm. The transfection efficiency was determined by the percentage of HA-positive macrophages. *E*, uptake of Lucifer yellow dye was assessed in WT MPM, *Akt3*$^{-/-}$ MPM (*KO*), and *Akt3*$^{-/-}$ MPMs transfected with Akt3 cDNA (*KO+Akt3*) for 48 h (*n* = 9). *F*, *Akt3*$^{-/-}$ MPM were transfected with control vector or Akt3 cDNA expression vector for 48 h. WT and transfected *Akt3*$^{-/-}$ MPMs were incubated without (control) or with 0.1 mg/ml of LDL for 24 h. Total cellular cholesterol was quantified using a Biovision Cholesterol/CE Quantitation Kit II (*n* = 8). *G*, Akt3 expression in human MDMs treated with control siRNA or Akt3 siRNA was assessed by Western blot analysis using rabbit anti-Akt3 and mouse anti-GAPDH antibodies (*n* = 6). *H*, foam cell formation assay of human MDMs treated with Akt3 siRNA and then cultured in the presence of 0.1 mg/ml native LDL for 48 h. Cells were fixed with 4% formaldehyde, stained with oil red O, and counterstained with hematoxylin. Quantification of macrophage foam cells was done as the percentage of the total number of cells (*n* = 6). Data represent means ± S.E. *, *p* < 0.05; *NS*, *p* > 0.05. Data are representative of at least three independent experiments.
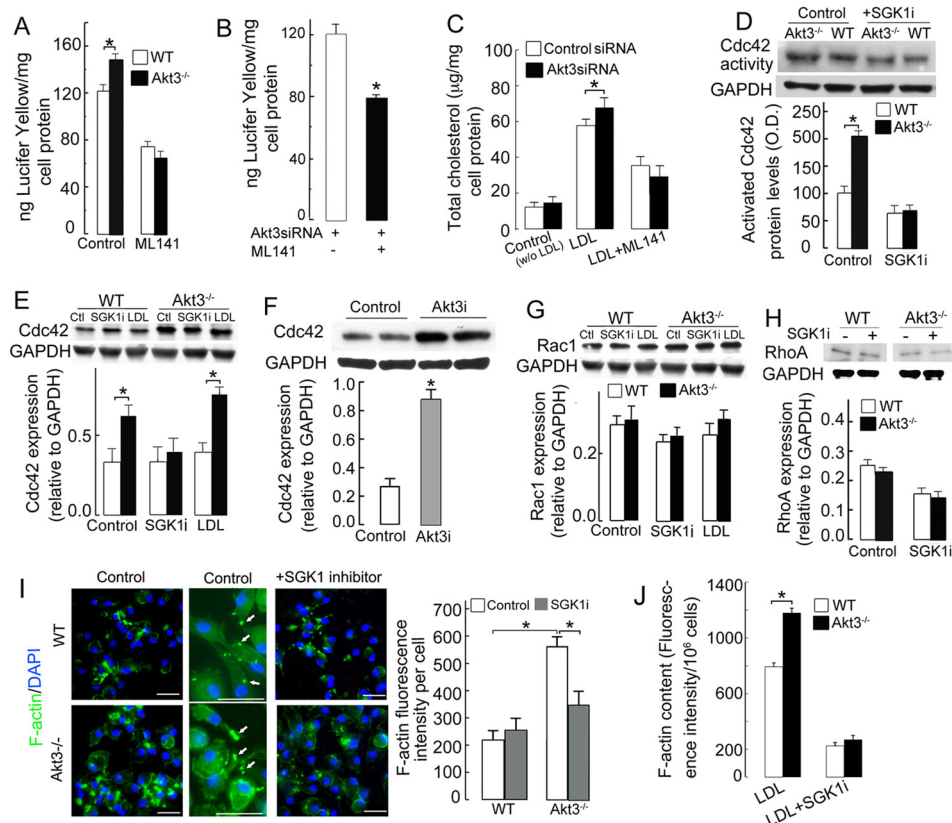
Figure 2. Akt3 inhibits macrophage pinocytosis of LDL and Lucifer yellow dye through actin-dependent macropinocytosis. *A*, uptake of Lucifer yellow dye by WT and *Akt3$^{-/-}$* MPMs. MPMs were cultured in 10% FBS/RPMI medium containing 0.5 mg/ml Lucifer yellow CH, 20 μM Src inhibitor (SU6656, *SU*), 10 μM cytochalasin D (*cytoD*), and 0.5 μM bafilomycin A1 (*Baf*) for 2 h. Then cells were washed and lysed, and uptake of Lucifer yellow was quantified by spectrofluorometry of the lysate (*n* = 6). *B*, human monocyte-derived macrophages were transfected with control or Akt3 siRNA and then incubated with 0.1 mg/ml LDL for 48 h in the presence or absence of the indicated inhibitors as in *A*. Lipids were extracted, and total cellular cholesterol was quantified using a Biovision Cholesterol/CE Quantitation Kit II (*n* = 6). Data represent means ± S.E. *, *p* < 0.05. Data are quantified from at least three independent experiments.

Figure 3. Increased activity of SGK1 promotes pinocytosis in *Akt3$^{-/-}$* macrophages. *A*, phosphorylation of Akt (Ser-473/Thr-308), total Akt, and Akt1/2 expression in WT and *Akt3$^{-/-}$* MPMs treated with 50 ng/ml M-CSF. *Ctl*, control without M-CSF treatment. *n* = 3. *B*, uptake of Lucifer yellow dye by WT and *Akt3$^{-/-}$* MPMs in the presence of 10 μM GSK3 inhibitor (*SB*), 20 nM mTOR inhibitor (*RAPA*), or 2 μM NFκB inhibitor (*BAY*). *n* = 8. *C*, phosphorylation and expression of NDRG1, an SGK1 specific substrate, in WT and *Akt3$^{-/-}$* MPMs assessed by Western blotting. *Bottom panel*, expression of SGK1 in WT and *Akt3$^{-/-}$* MPMs. *n* = 3. *D*, Lucifer yellow uptake by MPMs in the presence of SGK1 inhibitor (K-650394). *n* = 8. *E*, foam cell formation assay in WT and *Akt3$^{-/-}$* MPMs cultured in the presence of 1 mg/ml LDL and in the presence or absence of 25 μg/ml SGK1 inhibitor (SGK1i) for 24 h (*n* = 8). *F*, effect of SGK1 inhibitor (GSK-650394, 25 μg/ml) on the uptake of Lucifer yellow by WT and *Akt3$^{-/-}$* MPMs (*n* = 7). *G*, effect of Akt3 siRNA treatment on phosphorylation of NDRG1 and expression of NDRG1, Akt3, and Cdc42 in human MDMs assessed by Western blotting. GAPDH expression was used as a loading control (*n* = 6). *H*, uptake of Lucifer yellow dye by human MDM treated with control siRNA or Akt3 siRNA in the presence of 25 μg/ml SGK1i (*n* = 6). *I*, effect of 25 μg/ml SGKi on cholesterol accumulation in human MDM (*n* = 6). Human MDM were treated with Akt3 or control siRNA treatment and then cultured in the presence of 1 mg/ml LDL and 25 μg/ml SGK1i overnight, and cholesterol content was quantified. Data represent means ± S.E. *, *p* < 0.05. Data are representative of at least three independent experiments and are quantified from at least three independent experiments.

Figure 4. Akt3 inhibits macrophage pinocytosis via the SGK1/Cdc42 pathway. *A*, uptake of Lucifer yellow by WT and *Akt3*$^{-/-}$ MPMs in the presence or absence of 10 μM Cdc42 inhibitor (*ML141*). $n = 8$. *B*, uptake of Lucifer yellow dye by human MDMs treated with control siRNA or Akt3 siRNA in the presence of 10 μM ML141 ($n = 6$). *C*, cellular cholesterol levels of human MDMs treated with Akt3 siRNA or control siRNA in the presence of 1 mg/ml LDL and 10 μM ML141 ($n = 6$). *D*, Cdc42 activity in WT and *Akt3*$^{-/-}$ MPMs. Macrophages were treated with 25 μg/ml SGK1i overnight. Cells were then washed and lysed. Cdc42 activity in cell lysates was measured using a RhoA/Rac1/Cdc42 Activation Assay Combo Biochem Kit (Cytoskeleton) ($n = 3$). *E*, expression of Cdc42 in WT and *Akt3*$^{-/-}$ MPMs cultured in the presence or absence of 25 μg/ml SGK1i or 1 mg/ml LDL ($n = 3$). *F*, effect of suppression of Akt3 expression (siRNA treatment for 48 h, *Akt3i*) on Cdc42 expression in human MDM as assessed by Western blot analysis. GAPDH expression was used as a loading control ($n = 6$). *G*, expression of Rac1 in macrophages treated with 25 μg/ml SGK1 inhibitor and 0.8 mg/ml LDL (*top panel*). ($n = 3$). *H*, effect of SGK1i on RhoA expression in WT and *Akt3*$^{-/-}$ MPMs. Cells were incubated with or without 25 μg/ml SGK1i overnight. Cell protein samples were assessed by Western blot analysis. *I*, F-actin formation in WT and *Akt3*$^{-/-}$ MPMs exposed to 500 μ/ml LDL in the presence or absence (control) of SGK1 inhibitor. *Center panels*, F-actin formation (*white arrows*) at higher magnification. The actin cytoskeleton and the nuclei were visualized by staining with Alexa Fluor 488-phalloidin and DAPI, respectively. *Scale bars* = 25 μm, $n = 8$. *Right panels*, quantification of phalloidin fluorescence intensity. *J*, macrophages treated with 500 μg/ml LDL in the presence or absence of 25 μg/ml SGK inhibitor (GSK650394) for 4 h. Cells were stained with 0.6 μM TRITC-phalloidin. TRITC-phalloidin·F-actin complexes were extracted, and fluorescence was measured by SPECTRAmax GEMINI XS. Data represent means ± S.E. *, $p < 0.05$. Data are representative of at least three independent experiments.

cific phosphorylation substrate (29), was significantly increased in *Akt3*$^{-/-}$ MPMs, demonstrating enhanced SGK1 activity in these cells (Fig. 3*C*, *bottom panel*). Interestingly, NDRG1 expression was decreased in *Akt3*$^{-/-}$ MPMs compared with WT MPMs (Fig. 3*C*). K-650394, an inhibitor of SGK1, suppressed pinocytosis in *Akt3*$^{-/-}$ MPMs, having a significant effect on pinocytosis in WT MPMs (Fig. 3*D*). Importantly, the SGK1 inhibitor was able to prevent the excessive foam cell formation we observed in *Akt3*$^{-/-}$ MPMs incubated with native LDL (Fig. 3*E*). There was no significant effect of the SGK1 inhibitor on foam cell formation in WT MPMs (Fig. 3*E*), suggesting that, in Akt3-expressing cells, SGK1-dependent pinocytosis is suppressed. Indeed, the SGK1 inhibitor suppressed uptake of Lucifer yellow dye (a tracer for pinocytosis) in *Akt3*$^{-/-}$ MPMs but not in WT MPMs (Fig. 3*F*). We next tested whether Akt3 has an effect on SGK1 in human monocyte-derived macrophages. Knockdown of Akt3 by siRNA in human MDMs led to increased SGK1 activity (phospho-NDRG1/NDRG1 ratio) without inducing changes in SGK1 protein expression (Fig. 3*G*). Moreover, we observed that the SGK1

inhibitor eliminated the increased pinocytosis that was observed in human MDMs treated with Akt3 siRNA (Fig. 3, *H* and *I*). Taken together, these findings demonstrate that increased SGK1 activity mediates increased macropinocytosis in Akt3-deficient macrophages.

Cdc42 is involved in increased pinocytosis of *Akt3*$^{-/-}$ macrophages

Cdc42, a small GTPase of the Rho family, plays an important role in actin reorganization and polymerization and macropinocytosis (30). We tested whether Cdc42 is involved in increased macropinocytosis of *Akt3*$^{-/-}$ MPMs. ML141, an inhibitor of Cdc42, rendered pinocytosis similar in *Akt3*$^{-/-}$ and WT MPMs (Fig. 4*A*). In a similar fashion, the Cdc42 inhibitor inhibited excessive accumulation of either Lucifer yellow dye (Fig. 4*B*) or cholesterol derived from LDL (Fig. 4*C*) in human MDMs with suppressed expression of Akt3. Cdc42 activity and protein expression were increased in *Akt3*$^{-/-}$ MPMs (Fig. 4, *D* and *E*). We observed similar effects on Cdc42 in human MDMs with suppressed expression of Akt3 (Fig. 4*F*).
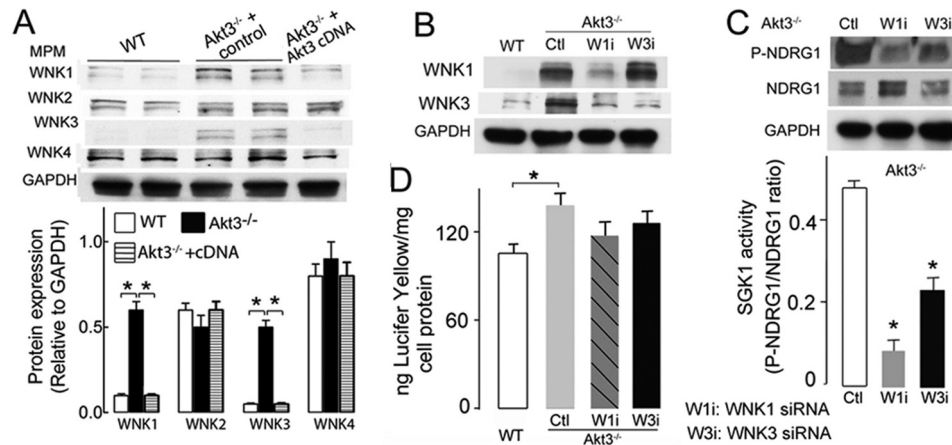
Figure 5. Increased expression of WNK1 and WNK3 may contribute to elevated SGK1 activity in *Akt3*$^{-/-}$ macrophages. *A*, expression of WNK1, WNK2, WNK3, and WNK4 in WT ($n = 5$) and *Akt3*$^{-/-}$ MPMs transfected with control ($n = 5$) or Akt3 cDNA ($n = 5$). *B*, WNK1 and WNK3 expression in WT or *Akt3*$^{-/-}$ macrophages treated with control (*Ctl*) or WNK1- or WNK3-specific siRNA ($n = 4$). *C*, phospho-NDRG1 and NDRG1 expression in *Akt3*$^{-/-}$ MPMs treated with control, WNK1, or WNK3 siRNA. SGK1 activity was calculated as phospho-NDRG1/NDRG1 ratio. $n = 4$. *, $p < 0.05$ *versus* control. *D*, pinocytosis of Lucifer yellow dye by WT, *Akt3*$^{-/-}$ (*Ctl*), and *Akt3*$^{-/-}$ MPMs treated with WNK1 siRNA (*W1i*) or WNK3 siRNA (*W3i*) ($n = 6$). Data represent means ± S.E. *, $p < 0.05$. Data are representative of at least three independent experiments and are quantified from at least three independent experiments.

Moreover, increased pinocytosis in these cells was normalized by the Cdc42 inhibitor (Fig. 4*B*). This increase in protein level of Cdc42 in *Akt3*$^{-/-}$ MPMs was abolished by the SGK1 inhibitor, indicating that Cdc42 is downstream of SGK1 (Fig. 4*E*). Interestingly, LDL enhanced SGK1 expression in *Akt3*$^{-/-}$ MPMs but not WT MPMs (Fig. 4*E*). Taken together, these data indicate that a lack of Akt3 in murine and human macrophages elevates pinocytosis of LDL through an SGK1/Cdc42 pathway.

Rac1 and RhoA are other major small GTPases of the Rho family involved in cytoskeletal rearrangements. In addition, Rac1 activates SGK1 in a PI3K-independent manner (31). To investigate whether Rac1 is involved in the activation of SGK1 in *Akt3*$^{-/-}$ MPMs, we assessed Rac1 expression in *Akt3*$^{-/-}$ MPMs. Western blot analysis showed that the Rac1 protein level is similar in WT and *Akt3*$^{-/-}$ macrophages, independent of preincubation with LDL, whereas its expression was slightly decreased in *Akt3*$^{-/-}$ macrophages treated with the SGK1 inhibitor (Fig. 4*G*, *top panel*). Rac1 activities were similar in WT and *Akt3*$^{-/-}$ MPMs (Fig. 4*G*, *bottom panel*). We also found no changes in the expression of RhoA (Fig. 4*H*). These data suggest that SGK1 and Cdc42 are the major players associated with enhanced pinocytosis in *Akt3*$^{-/-}$ MPMs.

F-actin assembly is suppressed in Akt3$^{-/-}$ macrophages

When cells were treated with native LDL in the presence of SGK1 inhibitor, F-actin assembly was reduced in *Akt3*$^{-/-}$ MPMs, whereas no significant change in WT MPM was observed (Fig. 4*I*), suggesting that SGK1 promotes F-actin formation in *Akt3*$^{-/-}$ macrophages.

Increased WNK1/WNK3 expression may contribute to enhanced SGK1 activity in murine macrophages

SGK1 can be activated by multiple kinases, including WNK family members (WNK1, WNK2, WNK3, and WNK4) (32, 33). It has been shown that SGK1 activity correlates with the expression of WNKs (33). Interestingly, WNKs are also substrates of Akt, providing a possible link between SGK1 and Akt kinases. We hypothesized that the expression of WNK family members

is modulated by the absence of Akt3, leading to changes in SGK1 activity. To test our hypothesis, we assessed the protein levels of WNK1–4 in WT and *Akt3*$^{-/-}$ MPMs by Western blot analysis. As shown in Fig. 5*A*, WNK1 and WNK3 levels are increased in *Akt3*$^{-/-}$ MPMs compared with WT MPMs, whereas the levels of WNK2 and WNK4 were similar in WT and *Akt3*$^{-/-}$ MPMs. To investigate whether Akt3 deficiency directly contributes to increased expression of WNK1 and WNK3, we overexpressed Akt3 in *Akt3*$^{-/-}$ MPMs and assessed WNK expression in these cells. Upon overexpression of Akt3, the protein levels of WNK1 and WNK3, but not of WNK2 or WNK4, decreased to a level that is comparable with WT MPMs (Fig. 5*A*). We next tested whether increased levels of WNK1 and WNK3 are mechanistically linked to SGK1 activation. Interestingly, knockdown of WNK1 with siRNA suppressed the expression of both WNK1 and WNK3 (Fig. 5*B*). This inhibition was associated with significantly decreased SGK1 activity (Fig. 5*C*). In contrast, knockdown of WNK3 in MPMs led to moderately decreased SGK1 activity in *Akt3*$^{-/-}$ MPMs with suppressed expression of WNK3 (Fig. 5*C*). Importantly, inhibition of WNK1 or WNK3 suppresses pinocytosis in *Akt3*$^{-/-}$ macrophages (Fig. 5*D*). These data indicate that Akt3 regulates the protein levels of WNK1 and WNK3 in macrophages, which, in turn, regulates SGK1 activity and pinocytosis via Cdc42 activity and actin assembly.

Discussion

Our study is the first to show that the Akt3/WNK axis acts as a negative regulator of actin-dependent macropinocytosis in murine and human macrophages. It demonstrates that dysregulation of this pathway may accelerate the accumulation of cholesterol in macrophages in a hyperlipidemic milieu. Our previous study of increased macrophage-dependent atherosclerosis in *Akt3*$^{-/-}$ macrophages and a parallel increase in non-receptor-mediated uptake of LDL by *Akt3*$^{-/-}$ macrophages indicates that the pathway is relevant *in vivo* (21).

The role of Akt kinases in pinocytosis has been studied previously, but not in an isoform-specific manner. The critical role

of phosphoinositide 3-kinases and Akt has been demonstrated in the *Dictyostelium* ameba, an organism with active macropinocytosis (23). Akt is recruited to inositol 1,4,5-trisphosphate-containing micropinosomes (34). The PI3K/Akt pathway also mediates pinocytosis in microglia (16). In macrophages, activation of mTORC1 by extracellular amino acids requires Akt-dependent macropinocytosis (35). On the other hand, M-CSF-induced macropinocytosis in macrophages was not affected by Akt inhibitor but was dependent on phospholipase C (PLC), Ras, and PKC activity (15). Macropinocytosis in bladder cancer cells was PI3K-dependent but Akt-independent (36). Thus, the Akt involvement in pinocytosis seems to be cell type- and stimulus-specific. We have recently demonstrated a specific macrophage-dependent atheroprotective role for Akt3 in hyperlipidemic ApoE$^{-/-}$ mice (21). Akt3 suppresses atherosclerosis by restricting cholesteryl ester accumulation and foam cell formation in macrophages. Mechanistic studies demonstrated that $Akt3^{-/-}$ macrophages accumulate cholesterol esters via two complementary mechanisms: increased lipoprotein uptake via pinocytosis and increased conversion of cholesterol into its storage form, cholesterol ester, because of an increased protein level of the cholesterol-esterifying enzyme ACAT1. This study elucidates the molecular pathway leading to increased pinocytosis in macrophages. It demonstrates that, although the PI3K/Akt pathway is considered a positive regulator of pinocytosis, there is a branch of this pathway that constitutively suppresses pinocytosis in macrophages and that deregulation of this branch leads to activation of pinocytosis.

Akt3 activity is regulated by several factors under physiological and pathological conditions, including sex hormones and microRNAs. Original studies of breast cancers showed that expression of Akt3 is greatly increased in estrogen receptor-deficient cancer cells (37), indicating that Akt3 expression may be negatively regulated by estrogen. Recent studies have shown that MiR-29 specifically inhibits Akt3 expression in BHK-21 cells and mouse skeletal muscle; however, its effect on Akt3 in macrophages is not known (38). Interestingly, miR-29 has been found to exert pro-atherosclerotic effects. Enhanced miR-29a levels were associated with an early stage of atherosclerosis (39). Sustained administration of locked nucleic acid (LNA)-miR-29, an miR-29 inhibitor, into an atherosclerotic mouse model improves indices of plaque morphology (40). Oxidized LDL in atherosclerotic lesions up-regulates miR-29b in human aortic smooth muscle cells (41). Other transcriptional regulators of miR-29s include inflammation-related genes, NFκB and CCAAT/enhancer-binding proteins (C/EBPs). Taking these finding into consideration, it is conceivable that constitutive (basal) Akt3 activity is regulated under physiologic and pathological conditions, particularly in proinflammatory conditions of atherosclerotic lesions, contributing to regulation of pinocytosis of LDL by macrophages and subsequent foam cell formation.

F-actin formation is the crucial step in pinocytosis (42). Several studies have shown that Akt regulates F-actin formation via small GTPases (Cdc42, Rac1, and RhoA) and Girdin/Akt-phosphorylation enhancer (43, 44). Akt activation promotes microglial pinocytosis induced by ATPγS, which contributes to Alzheimer's disease (16). Although the Akt isoform regulating F-actin is not known, it is likely that Akt1, a major Akt isoform, is expressed in most cells, including macrophages. This is in line with previous observations that $Akt1^{-/-}$ in macrophages is less efficient in uptake of LDL, even though the mechanism of reduced uptake has not been elucidated (21, 45). We found no increase in total Akt activity in the absence of Akt3, indicating that other isoforms of Akt are not activated as a compensatory mechanism. We also ruled out the idea that the major downstream targets of the Akt signaling pathway, including GSK3α, mTOR, and NFκB, were involved in increased pinocytosis in $Akt3^{-/-}$ macrophages. Instead, we demonstrated that, in the absence of Akt3, a close relative of Akt kinases, SGK1 kinase, is activated, leading to increased pinocytosis.

Akt and SGK kinases share similar downstream substrates and sometimes act redundantly in the control of signaling pathways (25). For example, elevated SGK1 activity contributes to resistance of breast cancer cells to Akt inhibitors (28). Our study demonstrates that the lack of activity of one specific member of Akt family in macrophages leads to increased SGK1 activity, overcompensating for a loss of Akt and leading to increased pinocytosis. SGK1 can be activated via Rac1 (31). However, we observed no increase in Rac1 expression or activity in the absence of Akt3, indicating that this pathway does not contribute to SGK1 activation in $Akt3^{-/-}$ macrophages. In contrast, we found that SGK1 is activated via WNK kinases. Similar to our observation in $Akt3^{-/-}$ macrophages, Wilson *et al.* (46) showed that phosphorylation of NDRG1 was elevated, whereas the NDRG1 level was decreased in insulin-induced mouse polarized kidney cortical collecting duct (mpkCCD) cells (46). Moreover, it was reported that phosphorylation of NDRG1 induces its degradation via proteasomal pathway (47); thus, it is likely that NDRG1 stability is reduced in $Akt3^{-/-}$ cells.

The WNK family of serine-threonine kinases is composed of four members: WNK1, WNK2, WNK3, and WNK4. WNK kinases play important roles in the regulation of electrolyte homeostasis, cell signaling, survival, and proliferation (48). Contribution of WNKs to fluid-phase pinocytosis has not been reported previously. Overexpression of the N termini of all four WNKs results in activation of SGK1 (33). In kidney epithelial cell line HEK293 cells, SGK1 was strongly activated by WNK1 and WNK4, whereas the effect of WNK2 and WNK3 on SGK1 activation was modest (33). Our study demonstrates that in $Akt3^{-/-}$ macrophages. WNK1 and WNK3, but not WNK2 or WNK4, promote activation of SGK1, indicating the cell specificity of the effect. Published data suggest that WNK3 is a phosphorylation substrate of Akt (49), whereas WNK1 is a substrate for both SGK1 and Akt, and both kinases can phosphorylate WNK1 at Thr-58/60 (50). It has been assumed that Akt2 and Akt3, but not Akt1, are responsible for WNK1 phosphorylation (51). Whether Akt3 regulates WNK1 and WNK3 expression through direct interaction (*e.g.* phosphorylation-induced degradation of WNK1 by Akt3) or through transcriptional, translational, and/or posttranslational regulation by Akt3-dependent signaling pathways is unknown. Additionally, whether Akt3 regulates WNK1 and WNK3 expression via the same mechanism is also unknown. Hence, the mechanism by which

ᔓASBMB

J. Biol. Chem. (2017) 292(22) 9283–9293 **9289**

loss of Akt3 leads to elevated WNK1 and WNK3 expression needs further investigation.

The Rho family GTPases (Cdc42, Rac1, and RhoA) are master regulators of actin assembly and subsequent pinocytosis. RhoA regulates actin-myosin contractility in the cell body, and its activity is associated with membrane protrusion, peripheral ruffles, and pinocytic vesicles (52–54). Rac1 activates macropinocytosis in many cell types, including neutrophils, dendritic cells, macrophages, podocytes, and fibroblasts, by stimulating F-actin-rich ruffle formation (55–58). Cdc42 has been shown to positively regulate macropinocytosis in macrophages and dendritic cells (59, 60). In this study, we observed that enhanced pinocytosis of $Akt3^{-/-}$ macrophages was suppressed by a Rac/Cdc42 inhibitor. Cdc42 expression and activity was increased in $Akt3^{-/-}$ macrophages, whereas no change in Rac1 expression or activity was observed, indicating that enhanced Cdc42 is responsible for increased F-actin formation and subsequent pinocytosis in $Akt3^{-/-}$ macrophages. The relationship between SGK1 and Cdc42 is still unknown. Our study suggests that SGK1 may activate Cdc42 by direct interaction with Cdc42. However, the mechanism by which SGK1 activates Cdc42 needs further investigation.

In sum, our study shows that, in macrophages, Akt3 suppresses expression of WNK1 and WNK3, which, in turn, restricts SGK1 activation and negatively controls Cdc42 activity and subsequent actin-dependent macropinocytosis of LDL. The finding that Akt3 inhibits foam cell formation via a specific pathway provides a promising new therapeutic target in atherosclerosis.

Experimental procedures

Materials

LDL was isolated and iodinated as described previously (61–63). Antibodies against Akt1, pan-Akt, phospho-Akt (Ser-473), phospho-Akt (Thr-308), phospho-NDRG1, NDRG1, HA tag, and WNK4 were purchased from Cell Signaling Technology. Antibodies against WNK1 were from GeneTex. Anti-Akt3 and anti-WNK2 were from Millipore and anti-GAPDH from Sigma. Anti-WNK3 antibody was purchased from Santa Cruz Biotechnology. The mTOR inhibitor (rapamycin) and NFκB inhibitors (BAY 11-7082) were from Calbiochem. The glycogen synthase kinase 3 (GSK3) inhibitor (SB 415286), V-ATPase inhibitor (bafilomycin A1), Lucifer yellow dye, Src inhibitor (SU6656), actin polymerization inhibitor (cytochalasin D), and Cdc42 inhibitor (ML141) were purchased from Sigma. The SGK1 inhibitor (GSK650394) was purchased from Santa Cruz Biotechnology. Mouse and human M-CSF were from eBioscience. Alexa Fluor 555-conjugated cholera toxin and TRITC-phalloidin were from Thermo Fisher Scientific.

Animal procedures

We used littermate-derived sex-, age-, and genetic background-matched mice in our experiments. $Akt3^{-/-}$ mice were generated as described previously (21). $Akt3^{-/-}$ mice were backcrossed ten or more times to C57Bl/6. After the final backcross, heterozygotes were mated to create background-matched wild-type and $Akt3^{-/-}$ mice for this study. MPMs were harvested from mice 3 days after intraperitoneal injection of thioglycolate. For each experiment, MPMs collected from three to five mice were mixed for treatments. We performed all procedures according to protocols approved by the Cleveland Clinic Institutional Animal Care and Use Committee (IACUC).

Human MDMs

All experiments performed with human blood were approved by the Institutional Review Board of the Cleveland Clinic. Informed consent was obtained in accordance with the Declaration of Helsinki. Monocytes were isolated from the blood of healthy donors ($n = 6$) by density centrifugation with Lymphoprep (Axis-Shield, Oslo, Norway) following the protocol of the manufacturer. The monocyte population was enriched by discarding non-adherent cells after 2 h incubation at 37 °C in a 5% CO_2 atmosphere. Monocytes were differentiated into macrophages by cultivation in RPMI 1640 medium containing 10% FBS and 50 ng/ml human M-CSF for 7 days.

In vitro cell-based assays

Isolation of thioglycolate-elicited MPMs and the ^{125}I-LDL cell association assay were performed as described previously (21). The foam cell formation assay was performed as follows. MPMs were cultured on glass slides in RPMI 1640/0.5% BSA and 1 mg/ml LDL for 24 h in the presence or absence of 25 μg/ml SGK1 inhibitor. Then the cells were fixed with 4% formaldehyde, stained with oil red O and counterstained with hematoxylin. The foam cell formation assay of human MDM was performed as follows. Human MDMs were treated with control or Akt3 siRNA and then incubated with 100 μg/ml of LDL for 48 h before fixation and oil red O staining, and quantification of macrophage foam cells was performed as described previously (21).

Pinocytosis assay

The pinocytic activity of macrophages was assessed as described before (64, 65). Briefly, Lucifer yellow CH (Sigma-Aldrich) was dissolved in 10% FBS/RPMI medium at 0.5 mg/ml. The Lucifer yellow medium was then added to macrophages that were cultured in 24-well plates (0.5 ml/well) in the presence of the indicated inhibitors. The plates were then either maintained on ice as a control or incubated at 37 °C for 2 h. The wells were drained and washed with PBS containing 1 mg/ml BSA three times and with PBS five times. After washing, cells were lysed by Triton X-100 (0.05%, 250 μl/well). Fluorescence of the lysate was read by SPECTRAmax GEMINI XS using excitation at 430 nm and emission at 540 nm.

Western blot analysis

MPMs were collected and plated in 6-well plates and synchronized by overnight serum depletion. Cells were then incubated with 10% FBS/RPMI containing 50 ng/ml M-CSF for 6 h before harvest. Cells were lysed in lysis buffer (Cell Signaling Technologies) with protease and phosphatase inhibitor (Roche). Equal amounts of lysate protein were separated by SDS-PAGE, blotted onto polyvinylidene difluoride membranes, and incubated with the corresponding antibodies. The specific signals were visualized by ECL substrate (Pierce). In a separate experiment, murine macrophages were treated with

SGK1 inhibitor for 24 h before harvest. Cells were collected and lysed. Expression of Cdc42 and RhoA was assessed by Western blot analysis.

Immunofluorescent staining of actin in macrophages

Immunofluorescent staining was performed as described previously (66). Briefly, peritoneal macrophages of WT and *Akt3*$^{-/-}$ mice were exposed to 500 μg/ml LDL in the presence or absence of 25 μg/ml SGK1 inhibitor (GSK650394) for 4 h. After treatment, cells were fixed, permeabilized, and stained with Alexa Fluor 488-conjugated phalloidin to visualize F-actin. The fluorescence intensity of F-actin was measured as a mean gray value using ImageJ software.

Cellular F-actin quantification

F-actin content was quantified by an adaptation of the methods described by Cano *et al.* (67) and Atkinson *et al.* (68). Cells were cultured in a 48-well plate and treated with 500 μg/ml LDL in RPMI/0.5% BSA medium in the presence or absence of 25 μg/ml SGK inhibitor (GSK650394) for 4 h. Thereafter, cells were fixed with 4% paraformaldehyde and stained for 2 h with a solution containing 0.6 μM TRITC-phalloidin and 0.5% Triton X-100 in PHEM (60 mM PIPES, 25 mM HEPES, 10 mM EGTA, and 2 mM MgSO4, pH 6.9) buffer. Cell solutions were collected and centrifuged at 80,000 rpm (346,000 × *g*) for 15 min at 4 °C (TL-100, Beckman Instruments, Inc.). The supernatant was discarded, and the pellets were extracted for 24 h in 500 μl of methanol. The fluorescence was read by SPECTRAmax GEMINI XS (excitation 540 nm, emission 575 nm).

siRNA transfection

Control and Akt3 siRNA were purchased from Santa Cruz Biotechnology. MISSION siRNA transfection reagent was from Sigma. Human monocytes were differentiated into macrophages by treatment with M-CSF. Human macrophages were treated with control siRNA or Akt3 siRNA according to the protocol of the manufacturer. After transfection, cells were used for an *in vitro* pinocytosis assay or Western blot analysis to assess expression of phospho-NDRG1, NDRG1, Akt, and Cdc42. In a separate experiment, murine macrophages were treated with control siRNA, WNK1 siRNA, or WNK3 siRNA in the presence of MISSION siRNA transfection reagent.

Akt3 cDNA transfection

Macrophages were transfected with control cDNA or Akt3-HA cDNA with jetPEI-Macrophage DNA transfection reagent (PolyPlus Transfection) for 24–48 h. After transfection, macrophages were used for the pinocytosis assay using Lucifer yellow dye, for immunofluorescent staining to determine the transfection efficiency, or for Western blot analysis to assess expression of the HA tag and WNK1–4.

Statistical analysis

All experiments were conducted two to three times, and representative results are presented. Data are presented as mean ± S.E. The statistical significance of differences was evaluated using Student's *t* test or Mann-Whitney *U* test. Significance was accepted at the level of $p < 0.05$. When multiple comparisons were made, a Bonferroni correction was made for each test.

References

1. Chimini, G., and Chavrier, P. (2000) Function of Rho family proteins in actin dynamics during phagocytosis and engulfment. *Nat. Cell Biol.* **2,** E191–E196
2. Kruth, H. S., Jones, N. L., Huang, W., Zhao, B., Ishii, I., Chang, J., Combs, C. A., Malide, D., and Zhang, W. Y. (2005) Macropinocytosis is the endocytic pathway that mediates macrophage foam cell formation with native low density lipoprotein. *J. Biol. Chem.* **280,** 2352–2360
3. Ferraro, D. A., Gaborit, N., Maron, R., Cohen-Dvashi, H., Porat, Z., Pareja, F., Lavi, S., Lindzen, M., Ben-Chetrit, N., Sela, M., and Yarden, Y. (2013) Inhibition of triple-negative breast cancer models by combinations of antibodies to EGFR. *Proc. Natl. Acad. Sci. U.S.A.* **110,** 1815–1820
4. Underhill, D. M., and Goodridge, H. S. (2012) Information processing during phagocytosis. *Nat. Rev. Immunol.* **12,** 492–502
5. Tabas, I., García-Cardeña, G., and Owens, G. K. (2015) Recent insights into the cellular biology of atherosclerosis. *J. Cell Biol.* **209,** 13–22
6. Greaves, D. R., and Gordon, S. (2009) The macrophage scavenger receptor at 30 years of age: current knowledge and future challenges. *J. Lipid Res.* **50,** S282–S286
7. Kruth, H. S. (2011) Receptor-independent fluid-phase pinocytosis mechanisms for induction of foam cell formation with native low-density lipoprotein particles. *Curr. Opin. Lipidol.* **22,** 386–393
8. Zhao, B., Li, Y., Buono, C., Waldo, S. W., Jones, N. L., Mori, M., and Kruth, H. S. (2006) Constitutive receptor-independent low density lipoprotein uptake and cholesterol accumulation by macrophages differentiated from human monocytes with macrophage-colony-stimulating factor (M-CSF). *J. Biol. Chem.* **281,** 15757–15762
9. Anzinger, J. J., Chang, J., Xu, Q., Buono, C., Li, Y., Leyva, F. J., Park, B. C., Greene, L. E., and Kruth, H. S. (2010) Native low-density lipoprotein uptake by macrophage colony-stimulating factor-differentiated human macrophages is mediated by macropinocytosis and micropinocytosis. *Arterioscler. Thromb. Vasc. Biol.* **30,** 2022–2031
10. Buono, C., Anzinger, J. J., Amar, M., and Kruth, H. S. (2009) Fluorescent PEGylated nanoparticles demonstrate fluid-phase pinocytosis by macrophages in mouse atherosclerotic lesions. *J. Clin. Invest.* **119,** 1373–1381
11. Levin, M. C., Jirholt, P., Wramstedt, A., Johansson, M. E., Lundberg, A. M., Trajkovska, M. G., Ståhlman, M., Fogelstrand, P., Brisslert, M., Fogelstrand, L., Yan, Z. Q., Hansson, G. K., Björkbacka, H., Olofsson, S. O., and Borén, J. (2011) Rip2 deficiency leads to increased atherosclerosis despite decreased inflammation. *Circ. Res.* **109,** 1210–1218
12. Choi, S. H., Harkewicz, R., Lee, J. H., Boullier, A., Almazan, F., Li, A. C., Witztum, J. L., Bae, Y. S., and Miller, Y. I. (2009) Lipoprotein accumulation in macrophages via toll-like receptor-4-dependent fluid phase uptake. *Circ. Res.* **104,** 1355–1363
13. Kruth, H. S. (2013) Fluid-phase pinocytosis of LDL by macrophages: a novel target to reduce macrophage cholesterol accumulation in atherosclerotic lesions. *Curr. Pharm. Des.* **19,** 5865–5872
14. Ghoshal, P., Singla, B., Lin, H., Feck, D. M., Cantu-Medellin, N., Kelley, E. E., Haigh, S., Fulton, D., and Csanyi, G. (2017) Nox2-mediated PI3K and cofilin activation confers alternate redox control of macrophage pinocytosis. *Antioxid. Redox Signal.* 10.1089/ars.2017.7059
15. Yoshida, S., Gaeta, I., Pacitto, R., Krienke, L., Alge, O., Gregorka, B., and Swanson, J. A. (2015) Differential signaling during macropinocytosis in response to M-CSF and PMA in macrophages. *Front. Physiol.* **6,** 8

16. Li, H. Q., Chen, C., Dou, Y., Wu, H. J., Liu, Y. J., Lou, H. F., Zhang, J. M., Li, X. M., Wang, H., and Duan, S. (2013) P2Y4 receptor-mediated pinocytosis contributes to amyloid β-induced self-uptake by microglia. *Mol. Cell. Biol.* **33,** 4282–4293

17. Vandermoere, F., El Yazidi-Belkoura, I., Demont, Y., Slomianny, C., Antol, J., Lemoine, J., and Hondermarck, H. (2007) Proteomics exploration reveals that actin is a signaling target of the kinase Akt. *Mol. Cell. Proteomics* **6,** 114–124

18. Rotllan, N., Chamorro-Jorganes, A., Araldi, E., Wanschel, A. C., Aryal, B., Aranda, J. F., Goedeke, L., Salerno, A. G., Ramírez, C. M., Sessa, W. C., Suárez, Y., and Fernández-Hernando, C. (2015) Hematopoietic Akt2 deficiency attenuates the progression of atherosclerosis. *FASEB J.* **29,** 597–610

19. Babaev, V. R., Hebron, K. E., Wiese, C. B., Toth, C. L., Ding, L., Zhang, Y., May, J. M., Fazio, S., Vickers, K. C., and Linton, M. F. (2014) Macrophage deficiency of Akt2 reduces atherosclerosis in Ldlr null mice. *J. Lipid Res.* **55,** 2296–2308

20. Manning, B. D., and Cantley, L. C. (2007) AKT/PKB signaling: navigating downstream. *Cell* **129,** 1261–1274

21. Ding, L., Biswas, S., Morton, R. E., Smith, J. D., Hay, N., Byzova, T. V., Febbraio, M., and Podrez, E. A. (2012) Akt3 deficiency in macrophages promotes foam cell formation and atherosclerosis in mice. *Cell Metab.* **15,** 861–872

22. Cohen, M. M., Jr. (2013) The AKT genes and their roles in various disorders. *Am. J. Med. Genet. A* **161A,** 2931–2937

23. Rupper, A., Lee, K., Knecht, D., and Cardelli, J. (2001) Sequential activities of phosphoinositide 3-kinase, PKB/Aakt, and Rab7 during macropinosome formation in *Dictyostelium*. *Mol. Biol. Cell* **12,** 2813–2824

24. Xue, G., and Hemmings, B. A. (2013) PKB/Akt-dependent regulation of cell motility. *J. Natl. Cancer. Inst.* **105,** 393–404

25. Bruhn, M. A., Pearson, R. B., Hannan, R. D., and Sheppard, K. E. (2010) Second AKT: the rise of SGK in cancer signalling. *Growth Factors* **28,** 394–408

26. Alessi, D. R., Pearce, L. R., and García-Martínez, J. M. (2009) New insights into mTOR signaling: mTORC2 and beyond. *Sci. Signal.* **2,** pe27

27. Firestone, G. L., Giampaolo, J. R., and O'Keeffe, B. A. (2003) Stimulus-dependent regulation of serum and glucocorticoid inducible protein kinase (SGK) transcription, subcellular localization and enzymatic activity. *Cell Physiol. Biochem.* **13,** 1–12

28. Sommer, E. M., Dry, H., Cross, D., Guichard, S., Davies, B. R., and Alessi, D. R. (2013) Elevated SGK1 predicts resistance of breast cancer cells to Akt inhibitors. *Biochem. J.* **452,** 499–508

29. Murray, J. T., Campbell, D. G., Morrice, N., Auld, G. C., Shpiro, N., Marquez, R., Peggie, M., Bain, J., Bloomberg, G. B., Grahammer, F., Lang, F., Wulff, P., Kuhl, D., and Cohen, P. (2004) Exploitation of KESTREL to identify NDRG family members as physiological substrates for SGK1 and GSK3. *Biochem. J.* **384,** 477–488

30. Higuchi, M., Masuyama, N., Fukui, Y., Suzuki, A., and Gotoh, Y. (2001) Akt mediates Rac/Cdc42-regulated cell motility in growth factor-stimulated cells and in invasive PTEN knockout cells. *Curr. Biol.* **11,** 1958–1962

31. Shelly, C., and Herrera, R. (2002) Activation of SGK1 by HGF, Rac1 and integrin-mediated cell adhesion in MDCK cells: PI-3K-dependent and -independent pathways. *J. Cell Sci.* **115,** 1985–1993

32. Lang, F., and Stournaras, C. (2013) Serum and glucocorticoid inducible kinase, metabolic syndrome, inflammation, and tumor growth. *Hormones* **12,** 160–171

33. Heise, C. J., Xu, B. E., Deaton, S. L., Cha, S. K., Cheng, C. J., Earnest, S., Sengupta, S., Juang, Y. C., Stippec, S., Xu, Y., Zhao, Y., Huang, C. L., and Cobb, M. H. (2010) Serum and glucocorticoid-induced kinase (SGK) 1 and the epithelial sodium channel are regulated by multiple with no lysine (WNK) family members. *J. Biol. Chem.* **285,** 25161–25167

34. Lee, S., Shen, Z., Robinson, D. N., Briggs, S., and Firtel, R. A. (2010) Involvement of the cytoskeleton in controlling leading-edge function during chemotaxis. *Mol. Biol. Cell* **21,** 1810–1824

35. Yoshida, S., Pacitto, R., Yao, Y., Inoki, K., and Swanson, J. A. (2015) Growth factor signaling to mTORC1 by amino acid-laden macropinosomes. *J. Cell Biol.* **211,** 159–172

36. Redelman-Sidi, G., Iyer, G., Solit, D. B., and Glickman, M. S. (2013) Oncogenic activation of Pak1-dependent pathway of macropinocytosis determines BCG entry into bladder cancer cells. *Cancer Res.* **73,** 1156–1167

37. Nakatani, K., Thompson, D. A., Barthel, A., Sakaue, H., Liu, W., Weigel, R. J., and Roth, R. A. (1999) Up-regulation of Akt3 in estrogen receptor-deficient breast cancers and androgen-independent prostate cancer lines. *J. Biol. Chem.* **274,** 21528–21532

38. Wei, W., He, H. B., Zhang, W. Y., Zhang, H. X., Bai, J. B., Liu, H. Z., Cao, J. H., Chang, K. C., Li, X. Y., and Zhao, S. H. (2013) miR-29 targets Akt3 to reduce proliferation and facilitate differentiation of myoblasts in skeletal muscle development. *Cell Death Dis.* **4,** e668

39. Huang, Y. Q., Cai, A. P., Chen, J. Y., Huang, C., Li, J., and Feng, Y. Q. (2016) The relationship of plasma miR-29a and oxidized low density lipoprotein with atherosclerosis. *Cell. Physiol. Biochem.* **40,** 1521–1528

40. Ulrich, V., Rotllan, N., Araldi, E., Luciano, A., Skroblin, P., Abonnenc, M., Perrotta, P., Yin, X., Bauer, A., Leslie, K. L., Zhang, P., Aryal, B., Montgomery, R. L., Thum, T., Martin, K., *et al.* (2016) Chronic miR-29 antagonism promotes favorable plaque remodeling in atherosclerotic mice. *EMBO Mol. Med.* **8,** 643–653

41. Chen, K. C., Wang, Y. S., Hu, C. Y., Chang, W. C., Liao, Y. C., Dai, C. Y., and Juo, S. H. (2011) OxLDL up-regulates microRNA-29b, leading to epigenetic modifications of MMP-2/MMP-9 genes: a novel mechanism for cardiovascular diseases. *FASEB J.* **25,** 1718–1728

42. Lavoie, J. N., Hickey, E., Weber, L. A., and Landry, J. (1993) Modulation of actin microfilament dynamics and fluid phase pinocytosis by phosphorylation of heat shock protein 27. *J. Biol. Chem.* **268,** 24210–24214

43. Qian, Y., Zhong, X., Flynn, D. C., Zheng, J. Z., Qiao, M., Wu, C., Dedhar, S., Shi, X., and Jiang, B. H. (2005) ILK mediates actin filament rearrangements and cell migration and invasion through PI3K/Akt/Rac1 signaling. *Oncogene* **24,** 3154–3165

44. Enomoto, A., Murakami, H., Asai, N., Morone, N., Watanabe, T., Kawai, K., Murakumo, Y., Usukura, J., Kaibuchi, K., and Takahashi, M. (2005) Akt/PKB regulates actin organization and cell motility via Girdin/APE. *Dev. Cell* **9,** 389–402

45. Fernández-Hernando, C., Ackah, E., Yu, J., Suárez, Y., Murata, T., Iwakiri, Y., Prendergast, J., Miao, R. Q., Birnbaum, M. J., and Sessa, W. C. (2007) Loss of Akt1 leads to severe atherosclerosis and occlusive coronary artery disease. *Cell Metab.* **6,** 446–457

46. Wilson, S. M., Mansley, M. K., Getty, J., Husband, E. M., Inglis, S. K., and Hansen, M. K. (2010) Effects of peroxisome proliferator-activated receptor gamma agonists on Na⁺ transport and activity of the kinase SGK1 in epithelial cells from lung and kidney. *Br. J. Pharmacol.* **159,** 678–688

47. Oh, Y. M., Park, H. B., Shin, J. H., Lee, J. E., Park, H. Y., Kho, D. H., Lee, J. S., Choi, H., Okuda, T., Kokame, K., Miyata, T., Kim, I. H., Lee, S. H., Schwartz, R. H., and Choi, K. (2015) Ndrg1 is a T-cell clonal anergy factor negatively regulated by CD28 costimulation and interleukin-2. *Nat. Commun.* **6,** 8698

48. Kahle, K. T., Ring, A. M., and Lifton, R. P. (2008) Molecular physiology of the WNK kinases. *Annu. Rev. Physiol.* **70,** 329–355

49. Garzon-Muvdi, T., Schiapparelli, P., ap Rhys, C., Guerrero-Cazares, H., Smith, C., Kim, D. H., Kone, L., Farber, H., Lee, D. Y., An, S. S., Levchenko, A., and Quiñones-Hinojosa, A. (2012) Regulation of brain tumor dispersal by NKCC1 through a novel role in focal adhesion regulation. *PLoS Biol.* **10,** e1001320

50. McCormick, J. A., and Ellison, D. H. (2011) The WNKs: atypical protein kinases with pleiotropic actions. *Physiol. Rev.* **91,** 177–219

51. Sanidas, I., Polytarchou, C., Hatziapostolou, M., Ezell, S. A., Kottakis, F., Hu, L., Guo, A., Xie, J., Comb, M. J., Iliopoulos, D., and Tsichlis, P. N. (2014) Phosphoproteomics screen reveals akt isoform-specific signals linking RNA processing to lung cancer. *Mol. Cell* **53,** 577–590

52. Kagaya, K., Watanabe, K., Fukazawa, Y., Suzuki, S., Kobayashi, M., Okawa, Y., Suzuki, M., Takahashi, H., Brummer, E., Kurita, N., Miyaji, M., and Stevens, D. A. (1992) Biochemical mechanisms of intracellular killing of fungi. *J. Med. Vet. Mycol.* **30,** Suppl. 1, 179–187

53. Palazzo, A. F., Cook, T. A., Alberts, A. S., and Gundersen, G. G. (2001) mDia mediates Rho-regulated formation and orientation of stable microtubules. *Nat. Cell. Biol.* **3,** 723–729

ASBMB

54. Fukata, Y., Oshiro, N., Kinoshita, N., Kawano, Y., Matsuoka, Y., Bennett, V., Matsuura, Y., and Kaibuchi, K. (1999) Phosphorylation of adducin by Rho-kinase plays a crucial role in cell motility. *J. Cell Biol.* **145,** 347–361

55. Fujii, M., Kawai, K., Egami, Y., and Araki, N. (2013) Dissecting the roles of Rac1 activation and deactivation in macropinocytosis using microscopic photo-manipulation. *Sci. Rep.* **3,** 2385

56. West, M. A., Prescott, A. R., Eskelinen, E. L., Ridley, A. J., and Watts, C. (2000) Rac is required for constitutive macropinocytosis by dendritic cells but does not control its downregulation. *Curr. Biol.* **10,** 839–848

57. Chung, J. J., Huber, T. B., Gödel, M., Jarad, G., Hartleben, B., Kwoh, C., Keil, A., Karpitskiy, A., Hu, J., Huh, C. J., Cella, M., Gross, R. W., Miner, J. H., and Shaw, A. S. (2015) Albumin-associated free fatty acids induce macropinocytosis in podocytes. *J. Clin. Invest.* **125,** 2307–2316

58. Ridley, A. J., and Hall, A. (1992) The small GTP-binding protein rho regulates the assembly of focal adhesions and actin stress fibers in response to growth factors. *Cell* **70,** 389–399

59. Kerr, M. C., and Teasdale, R. D. (2009) Defining macropinocytosis. *Traffic* **10,** 364–371

60. Harris, K. P., and Tepass, U. (2010) Cdc42 and vesicle trafficking in polarized cells. *Traffic* **11,** 1272–1279

61. Podrez, E. A., Schmitt, D., Hoff, H. F., and Hazen, S. L. (1999) Myeloperoxidase-generated reactive nitrogen species convert LDL into an atherogenic form *in vitro*. *J. Clin. Invest.* **103,** 1547–1560

62. Mc, F. A. (1958) Efficient trace-labelling of proteins with iodine. *Nature* **182,** 53

63. Bilheimer, D. W., Eisenberg, S., and Levy, R. I. (1972) The metabolism of very low density lipoprotein proteins: I: preliminary *in vitro* and *in vivo* observations. *Biochim. Biophys. Acta* **260,** 212–221

64. Swanson, J. A., Yirinec, B. D., and Silverstein, S. C. (1985) Phorbol esters and horseradish peroxidase stimulate pinocytosis and redirect the flow of pinocytosed fluid in macrophages. *J. Cell Biol.* **100,** 851–859

65. Burgdorf, S., Kautz, A., Böhnert, V., Knolle, P. A., and Kurts, C. (2007) Distinct pathways of antigen uptake and intracellular routing in CD4 and CD8 T cell activation. *Science* **316,** 612–616

66. Rivière, J. B., van Bon, B. W., Hoischen, A., Kholmanskikh, S. S., O'Roak, B. J., Gilissen, C., Gijsen, S., Sullivan, C. T., Christian, S. L., Abdul-Rahman, O. A., Atkin, J. F., Chassaing, N., Drouin-Garraud, V., Fry, A. E., Fryns, J. P., *et al.* (2012) *De novo* mutations in the actin genes ACTB and ACTG1 cause Baraitser-Winter syndrome. *Nat. Genet.* **44,** 440–444

67. Cano, M. L., Lauffenburger, D. A., and Zigmond, S. H. (1991) Kinetic analysis of F-actin depolymerization in polymorphonuclear leukocyte lysates indicates that chemoattractant stimulation increases actin filament number without altering the filament length distribution. *J. Cell Biol.* **115,** 677–687

68. Atkinson, S. J., Hosford, M. A., and Molitoris, B. A. (2004) Mechanism of actin polymerization in cellular ATP depletion. *J. Biol. Chem.* **279,** 5194–5199